Published in final edited form as:
Meas Sci Technol. 2014 September 1; 25(9): . doi:10.1088/0957-0233/25/9/095201.

Model-Based, Closed-Loop Control of PZT Creep for Cavity Ring-Down Spectroscopy

A D McCartt[1,2], **T J Ognibene**[2], **G Bench**[2], and **K W Turteltaub**[3]

A D McCartt: mccartt@stanford.edu

[1]Department of Mechanical Engineering, Stanford University, USA

[2]Center for Accelerator Mass Spectrometry, Lawrence Livermore National Lab, USA

[3]Biology and Biotechnology Division, Lawrence Livermore National Lab, USA

Abstract

Cavity ring-down spectrometers typically employ a PZT stack to modulate the cavity transmission spectrum. While PZTs ease instrument complexity and aid measurement sensitivity, PZT hysteresis hinders the implementation of cavity-length-stabilized, data-acquisition routines. Once the cavity length is stabilized, the cavity's free spectral range imparts extreme linearity and precision to the measured spectrum's wavelength axis. Methods such as frequency-stabilized cavity ring-down spectroscopy have successfully mitigated PZT hysteresis, but their complexity limits commercial applications. Described herein is a single-laser, model-based, closed-loop method for cavity length control.

Keywords

PZT; creep; control; cavity; CRDS; spectroscopy

1. Introduction

Starting with cavity ring-down spectroscopy's nascent experiments involving mirror reflectivity, the technique has focused on the sensitivity of cavity-based optical-methods [1, 2]. High-finesse cavities eventually allowed for effective optical-path-lengths on the order of a few kilometers. Initial cavity ring-down spectroscopy (CRDS) experiments attempted to harness this sensitivity [3–10]. In this pursuit, experimental concessions were occasionally made that undermined other beneficial features of CRDS. Specifically, cavity lengths were modulated to increase the ring-down rate and simplify the implementation of new laser sources [11, 12]. While this modification allowed for compact spectroscopic devices with unprecedented levels of sensitivity, these CRDS systems could no longer utilize the precise free spectral range (FSR) of a high-finesse cavity.

When properly mode matched, a high-finesse cavity's transmission spectrum is a "comb" of FSR spaced resonant peaks. In order to obtain sub-FSR resolution spectra, the cavity length must be adjusted to shift the wavelength of the "comb" peaks. Simply adjusting the voltage

of a cavity PZT to a given value will not properly set and stabilize the cavity length. PZT hysteresis affects the accuracy and precision of cavity length control. The non-linearity of PZT actuation is well documented, however of equal importance in this implementation are PZT-creep effects [13, 14]. When the PZT is set to a new voltage, PZT creep will continuously alter the cavity length. In order to utilize the FSR's precision, the cavity length must be stabilized with a reference. Frequency-stabilized cavity ring-down spectroscopy (FS-CRDS) typically employs a reference laser to maintain the cavity length [15]. While FS-CRDS provides excellent wavelength measurement linearity and resolution, its complexity hinders commercial applications.

This paper describes a model-based, closed-loop method to control PZT creep induced changes to cavity-length. Using feedback from the spectroscopic features of an absorbing test gas and a logarithmic PZT-voltage diver function, the effects of PZT creep can be removed from the CRDS measurement. Unlike FS-CRDS this method is easily implemented and viable for commercial instruments.

2. Instrument Design

A heavily modified Picarro (Santa Clara, CA) mid-IR CRDS system was used for all experiments reported in this paper[16]. The Picarro system utilizes a Hamamatsu quantum cascade laser (QCL), an etalon-based wavelength monitor, and a high-finesse ring-cavity. The QCL uses single phonon-continuum depopulation and distributed feedback structures to produce a continuous-wave light source near 2190 cm^{-1}. The QCL is capable of tuning over a 5 cm^{-1} region. The length of the cavity is modulated by a PZT stack attached to the rear mirror. This simple and robust design is field deployable and commercially proven.

Several significant modifications were made to the picarro system. Instead of an acousto-optic modulator (AOM), a Faraday isolator was used to prevent feedback into the QCL. Extra care was taken to stabilize the temperature and pressure of the cavity. The cavity was encased in 25 cm of insulation and pressure leaks were reduced to less than 1 Pascal an hour. Thermal expansion and pressure induced mechanical stress can alter the length of the cavity. These modifications mitigated these cavity length altering factors and facilitated accurate spectroscopic measurements.

3. CRDS Data Acquisition Methods

3.1. Cavity Tuning

The continuous-wave CRDS (CW-CRDS) data acquisition method, first described in Romanini et al. and later utilized in most commercial instruments, constantly modulates the cavity transmission spectrum over a continuous-wave, laser-light source [11]. Typically a PZT is attached to one of the cavity mirrors to dither the cavity length. A detector is placed in the path of the laser beam exiting the cavity. When cavity laser light injection exceeds a pre-defined threshold measured by the detector, the laser source is turned off. The detector then records the decay of light leaked out of the cavity (the "ring-down") in order to quantify the loss of the cavity and test gas. This all occurs while the cavity transmission spectrum is modulated about the laser light source. Because the cavity length is constantly

modulated, the cavity FSR cannot be used for a relative frequency reference, and an additional wavelength measurement system must be employed. Traditionally, an etalon-based system is used to measure the wavelength of ring-down events, but extremely accurate, direct-frequency-comb systems have been utilized [17]. When spectroscopic features of interest are large enough to serve as an absolute wavelength reference, etalon measurements systems are more than adequate. However, when attempting to measure smaller spectroscopic peaks, particularly when located on the “wing” of larger spectroscopic features, etalon wavelength measurement drift due to temperature and laser pointing effects can degrade sensitivity and accuracy.

3.2. Laser Current Tuning

This paper’s elected method of CRDS data acquisition does not modulate the cavity length. Instead, the transmission comb is set to a wavelength of interest and cavity laser light injection is achieved through current manipulation. Once cavity resonance is attained, the laser is switched off, the ring-down is recorded, and then the process is repeated as desired. In order to achieve sub-FSR wavelength resolution, the cavity length must be adjusted. See Figure 1 below for a graphical representation. The different cavity lengths produces multiple, uniformly-spaced, FSR comb spectra, which are interpolated and fit to a spectroscopic model. The cavity FSR imparts extreme linearity and precision to the measured CRDS frequency axis. An etalon-based wavelength monitor aids in the correct binning of ring-down events into the proper comb peaks, however binning can be accomplished with laser current and temperature data alone. When fitting the FSR comb spectra to the model, the relative spacing between peaks is set while the wavelength offset of a “comb” spectra is a free parameter. This fit determines the control parameters to correctly compensate for the PZT displacement hysteresis loop. PZT creep is suppressed by an additional control loop discussed below.

4. Experiment Description: PZT Creep Mitigation

Laser current tuning CRDS requires a wavelength or position reference to stabilize the length of the cavity. For the method described here, the contours of a spectroscopic feature are used as a wavelength reference. In order to clearly present the experimental method, a strong, relatively uncrowded P(35) nitrous oxide ro-vibrational transition of the fundamental vibrational band was selected for all data presented here. The test gas contained trace amounts of nitrous oxide in nitrogen (~100 ppb) at total pressures near 70 Torr.

In order to elucidate the negative effects of PZT creep on CRDS, a simple step change PZT voltage profile with 18 discrete steps was used to measure the nitrous oxide antisymmetric stretch band P(35) peak. At each discrete voltage step, 1000 ring-downs were collected. Figure 2 plots the measured nitrous oxide loss versus an etalon-based wavenumber measurement. The PZT step-change profile allows for multiple ring-down clusters to be taken of the P(35) peak at sub-FSR resolution[‡]. The inset shows the loss time history of ring-downs from a single PZT voltage value. The loss time history of a PZT-step change can

[‡]The cavity used in this paper had an FSR of .0150065(5) cm^{-1} for the measurement wavelength region.

be accurately modeled by a logarithmic function. This phenomenon is deleterious to sensitivity and indicative of PZT creep [13, 14].

The cavity length can be accurately estimated from peak Voigt fits. Measured spectra are fit, and the resultant spectroscopic model is used to convert loss to resonant cavity wavelength (cavity length). For the purposes of cavity length stabilization described below, the only necessary information is a first-order approximation of the change in cavity length with respect to loss at a given wavelength. This can be accurately calculated from the spectroscopic model, but could also be determined from a simple interpolation of the test data. Sensitivity is improved by using ring-down clusters located in dynamic loss regions such as those in the inset of Figure 2. Peaks separated by $n+\frac{1}{2}$ FSR provide ideal spectra for loss to length sensitivity[§].

Equation (1) can accurately model the cavity-length time history after a PZT step change [13, 14].

$$\mathrm{L(t)=L_o}\left[1+\gamma\log_{10}\left(\frac{\mathrm{t}}{\mathrm{t_o}}\right)\right] \quad (1)$$

L_o is a constant defined by the cavity length at time t_o after the PZT step change, and γ is a creep factor that determines the rate of PZT drift.

A model-based, closed-loop control method can suppress PZT creep using the estimated cavity length in the form of the fitted parameters from Equation 1. The method described here relies on a voltage control function shown in Equation 2.

$$\mathrm{V(t)=Vo}\left[1+\gamma_{\mathrm{v}}\log_{10}\left(\frac{\mathrm{t}}{\mathrm{t_o}}\right)\right] \quad (2)$$

Jung et al. first used Equation 2 for open-loop, PZT-creep control [18]. In this “model-based, closed-loop” experiment the parameters of Equation 2 are constantly updated by a feedback loop depicted in Figure 3. The loss time histories of each discrete cavity length are fit with Equation 1.

The creep factor γ of Equation 1 is then used to adjust the voltage creep factor γ_v in Equation 2. Because the desired output is $\gamma = 0$, the control loop is inherently stable (negative feedback), and adaptive control techniques that scale the loop gain with the magnitude of γ are well suited for this method. The cavity length offset (L_o) is adjusted by a separate FSR-comb fit described above. This process is repeated for each voltage step. These parameters are each entered into Equation 2 and combined to create a piecewise, PZT-voltage profile. Collecting new loss time histories with this voltage profile closes the feedback loop.

[§]where n is an integer

In practice, spectroscopic data is taken in between creep data for each cavity length of a measurement routine. Figure 4 shows how spectra and creep-fit data are acquired for a single, creep-controlled, PZT-voltage step. The initial creep-drift effects are recorded after the voltage step change occurs. After a predetermined amount of time (5 ms in Figure 4) the laser tunes to other peaks in the cavity transmission comb to obtain the surrounding spectra. After recording spectra from the desired regions, the laser returns to the PZT-creep fit cavity-transmission peak to record additional data before transitioning to the next PZT voltage step. In this way, the maximum amount of time is allotted to observe PZT drift, and the most accurate adjustment can be fed to the control loop.

5. Results

Figure 5 below compares PZT voltage profiles and their resultant loss time histories for experiments with and without PZT-creep compensation. Both loss columns are from measurements of the P(35) nitrous oxide peak. The panels on the left represent an experiment with PZT creep. The PZT was actuated with a simple step-change voltage profile, and the measured loss clearly displayed PZT-creep effects. The panels on the right represent an experiment without PZT creep. The upper-right panel of Figure 5 depicts the piecewise, logarithmic voltage-profile described above, and the corresponding loss measurement does not show drift from PZT creep.

The step with the highest voltage exhibited the most extreme creep effects. Histograms representing this region for both experiments are plotted in Figure 6 below. These histograms represent the cavity-length deviation from mean as determined by fitting the loss data to a spectroscopic model. Each count represents a single ring-down event, and the histogram interval size is set to twice the limit of quantification. The etalon-based wavelength monitor could not measure a statistically-significant difference between the two experimental procedures.

6. Discussion

The results above clearly demonstrate the effectiveness of the model-based, closed-loop, PZT-creep control method. Without PZT-creep compensation, 100 nanometer cavity-length drift was routinely observed[‖]. The benefits of laser-current-tuning data acquisition outlined above would be greatly degraded without PZT-creep compensation. The negative effects of creep drift are not limited to wavelength measurement accuracy. Given that the length measurements in Figure 6 are derived from loss, the histogram profiles substantiate the sensitivity advantages of the model-based, closed-loop method.

PZT-creep compensation parameters are specific to each laser-current-tuning, data-acquisition routine. These parameters are determined iteratively to compensate for hysteresis. Due to the time-history dependence and long duration of a single feedback-loop iteration, state space analysis was not practical. However, as was found in Jung et al., the values of these creep parameters are repeatable for a given PZT time history [14]. Once a system had converged, only small variations in creep parameters were observed.

[‖]equivalent to a 5×10^{-4} cm^{-1} change in resonant wavenumber

Nonetheless, changes to the test gas can alter the duration of the data acquisition routine and affect PZT-creep compensation. The model-based, closed-loop control can deal with such eventualities, but cavity length stability should be monitored for disturbances. Large disturbances may require the user to wait for the creep compensation parameters to re-converge. However, most large disturbances indicate an inefficient data acquisition routine that should be replaced.

For completely unknown test gas compositions, this method is reduced to open-loop control. For closed-loop control, the only requirement is a spectroscopic feature with a large loss-to-wavelength derivative that can be used as a cavity-length reference. Knowledge of the exact test gas composition is not required. However, the species of the spectroscopic feature selected for cavity-length reference must be present at levels adequate to resolve and compensate for PZT creep. Similar a priori knowledge of the test gas composition is often required of commercial CRDS systems, which are typically designed to measure specific isotopic or species concentrations.

This data acquisition method requires an accurate spectroscopic model for proper implementation. This model can be solved iteratively with the PZT-creep compensation parameters, but the model parameter results will only be as accurate as the selected model components. Furthermore, when fitting peaks that exhibit physical characteristics not captured by a Voigt profile, such as Dicke narrowing, convergence will be slow, and results for dependent parameter pairs will be inaccurate (e.g. pressure broadening and Dicke narrowing). For these cases, it is recommended to initially characterize the spectroscopic model using an instrument with an independent means of wavelength measurement (FS-CRDS, cavity-enhanced direct frequency comb spectroscopy (CE-DFCS), etc.). However with accurate reference standards for calibration, these more complicated CRDS systems are not necessary to accurately quantify species concentrations.

More accurate models of PZT creep exist in the literature and could be implemented with this model-based, closed-loop control method[19, 20]. However, the logarithmic PZT-creep model was selected for several reasons. First, while the logarithmic model is not capable of capturing the entire PZT-creep phenomena from voltage step change to drift rates at long times, it is capable of accurately modeling PZT drift after the large initial translation from the step change. Modeling the long-term PZT-drift data alone is adequate for the model-based, closed-loop control method, and in fact, the data acquisition rate of the CRDS system cannot reliably resolve the initial translation. Application of more complex models to the long-term PZT-drift segment of the data opens avenues to spurious solutions that do not represent physical phenomena. Furthermore, the difficulty of inverting the models for PZT control increases with model complexity. Using the logarithmic model, with only two parameters, simplifies implementation and expedites convergence.

This method was designed to enable the precise measurement of relatively small peaks located on the wings of larger spectroscopic features. The stabilized cavity comb allows CRDS measurements to be made at a precise relative wavelength on the wing of the larger peak. Because PZT creep is a long-term phenomenon which requires tens of seconds to accurately characterize, total measurement time is on the order of minutes for data

acquisition routines with multiple cavity lengths, and the method is primarily suited for sensitive measurements requiring longer averaging times.

The method presented here garners many of the benefits of FS-CRDS without the complexity. The onus of cavity length stabilization is transferred from an additional experimental apparatus to software routines. It by no means replaces FS-CRDS or CE-DFCS, but the simplicity of the method is well suited for commercial applications.

Acknowledgments

Work performed (partially) at the Research Resource for Biomedical AMS, which is operated at LLNL under the auspices of the U.S. Department of Energy under contract DE-AC52-07NA27344. The Research Resource is supported by the National Institutes of Health, National Center for Research Resources, Biomedical Technology Program grant #P41 RR13461. This project was funded, in part, by LLNL's Laboratory Directed Research and Development (LDRD) program. ADM was supported by the Lawrence Scholar Program. ADM would like to thank Prof. Ronald Hanson and Dr. Jay Jeffries. The authors would also like to thank Picarro for its collaborative efforts, Dr. Sze Tan for sharing his critical hardware knowledge, Dr. John Hoffnagle for his astute feedback, and Dr. Eric Crosson for his continuous support.

References

1. Herbelin JM, McKay JA. Development of laser mirrors of very high reflectivity using the cavity-attenuated phase-shift method. Applied optics. Oct; 1981 20(19):3341–4. [PubMed: 20333153]
2. Anderson DZ, Frisch JC, Masser CS. Mirror reflectometer based on optical cavity decay time. Applied optics. Apr.1984 23(8):1238. [PubMed: 18204709]
3. O'Keefe, Anthony; Deacon, David AG. Cavity ring-down optical spectrometer for absorption measurements using pulsed laser sources. Review of Scientific Instruments. 1988; 59(12):2544.
4. O'Keefe A, Scherer JJ, Cooksy AL, Sheeks R, Heath J, Saykally RJ. Cavity ring down dye laser spectroscopy of jet-cooled metal clusters: Cu2 and Cu3. Chemical Physics Letters. Sep; 1990 172(3–4):214–218.
5. Romanini D, Lehmann KK. Ring-down cavity absorption spectroscopy of the very weak HCN overtone bands with six, seven, and eight stretching quanta. The Journal of Chemical Physics. 1993; 99(9):6287.
6. Yu T, Lin MC. Kinetics of phenyl radical reactions studied by the cavity-ring-down method. Journal of the American Chemical Society. 1993; 115(10):4371–4372.
7. Romanini, Daniele; Lehmann, Kevin K. Cavity ring-down overtone spectroscopy of HCN, H13CN and HC15N. The Journal of Chemical Physics. 1995; 102(2):633.
8. Scherer JJ, Voelkel D, Rakestraw DJ. Infrared cavity ringdown laser absorption spectroscopy (IR-CRLAS). Chemical Physics Letters. 1995; 2614(October)
9. Jongma, Rienk T.; Boogaarts, Maarten GH.; Holleman, Iwan; Meijer, Gerard. Trace gas detection with cavity ring down spectroscopy. Review of Scientific Instruments. 1995; 66(4):2821.
10. Zalicki, Piotr; Zare, Richard N. Cavity ring-down spectroscopy for quantitative absorption measurements. The Journal of Chemical Physics. 1995; 102(7):2708.
11. Romanini D, Kachanov AA. CW cavity ring down spectroscopy. Chemical Physics Letters. 1997; 264(3–4):316–322.
12. Romanini D, Kachanov AA, Stoeckel F. Diode laser cavity ring down spectroscopy. Chemical Physics Letters. 1997; 270(5–6):538–545.
13. Jung, Hewon; Gweon, Dae-Gab. Creep characteristics of piezoelectric actuators. Review of Scientific Instruments. 2000; 71(4):1896.
14. Jung, Hewon; Shim, Jong Youp; Gweon, DaeGab. Tracking control of piezoelectric actuators. Nanotechnology. Mar; 2001 12(1):14–20.
15. Hodges, Joseph T.; Layer, Howard P.; Miller, William W.; Scace, Gregory E. Frequency-stabilized single-mode cavity ring-down apparatus for high-resolution absorption spectroscopy. Review of Scientific Instruments. 2004; 75(4):849.

16. Du, Xu; Farinas, Alejandro D.; Crosson, Eric R.; Balslev-Clausen, David; Blunier, Thomas. Development of a field-deployable isotopic N2O analyzer based on mid-infrared cavity ring-down spectroscopy. Proc SPIE. 2011; 8032:803207.

17. Thorpe MJ, Ye J. Cavity-enhanced direct frequency comb spectroscopy. Applied Physics B. May; 2008 91(3–4):397–414.

18. Jung, Hewon; Shim, JY.; Gweon, DG. New open-loop actuating method of piezoelectric actuators for removing hysteresis and creep. Review of Scientific Instruments. 2000; 71(9):3436.

19. Liu, Yanfang; Shan, Jinjun; Qi, Naiming. Creep modeling and identification for piezoelectric actuators based on fractional-order system. Mechatronics. Oct; 2013 23(7):840–847.

20. Kuhnen, Klaus; Krejci, Pavel. Compensation of complex hysteresis and creep effects in piezoelectrically actuated systems-a new Preisach modeling approach. Automatic Control, IEEE Transactions on. 2009; 54(3):537–550.

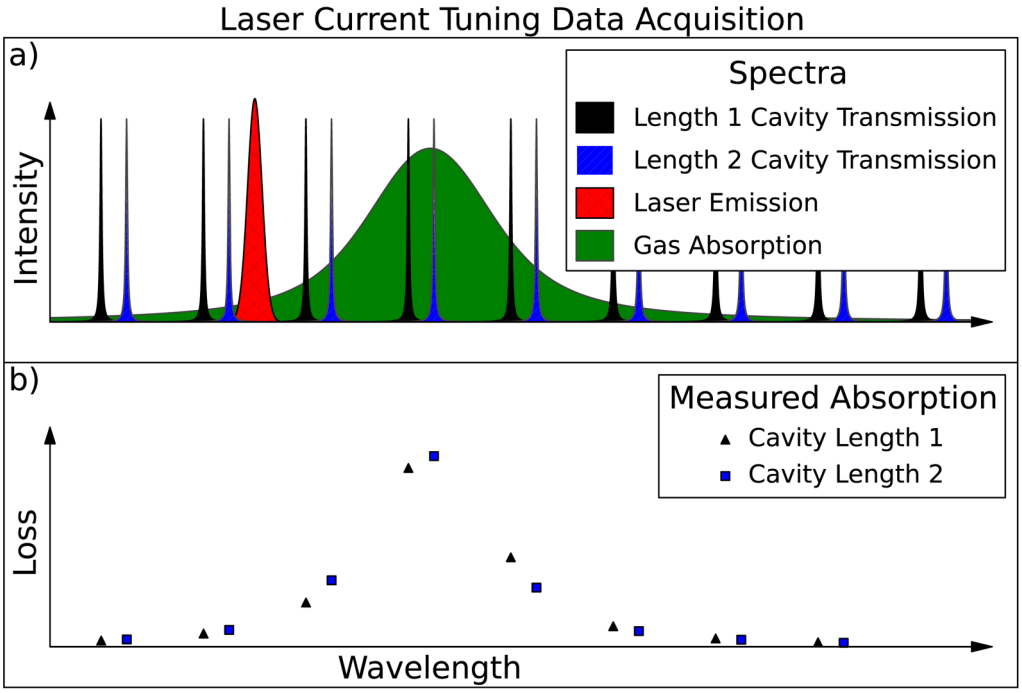

Figure 1.

Graphical depiction of CRDS data acquisition method utilized in this paper. Inset a), the laser emission spectrum is modulated over a peak of the cavity transmission spectrum until the desired number of ring-downs are collected. The temperature of the laser is then altered to shift the emission spectrum to another cavity transmission peak and the process is repeated. Once all of the data points for a given cavity length are collected, the ring-downs are grouped into peak-bins and averaged. The cavity length is then shifted and the entire process repeated. Inset b) shows the FSR spaced spectra from two cavity length transmission combs.

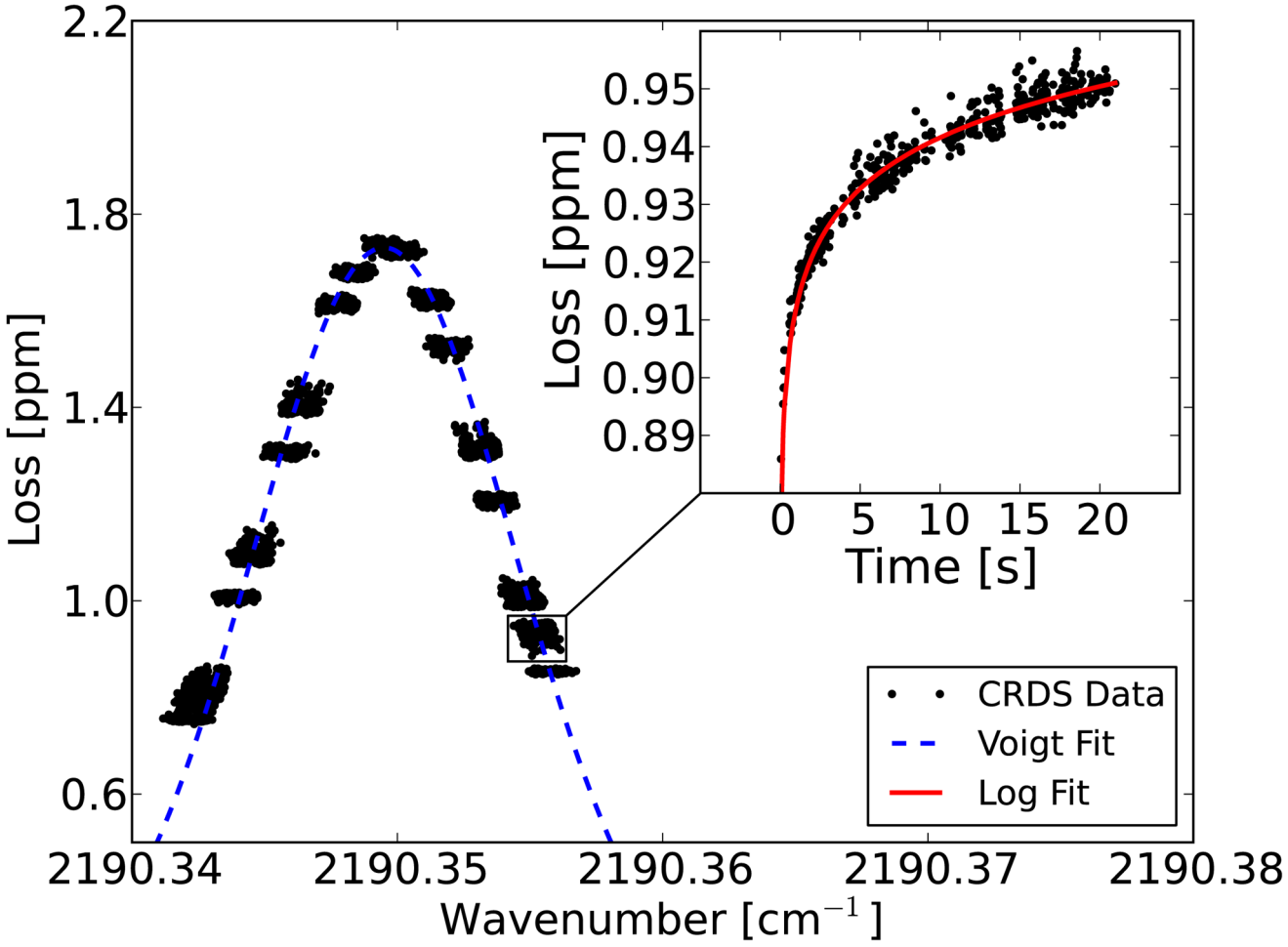

Figure 2.
Spectra with PZT Creep.

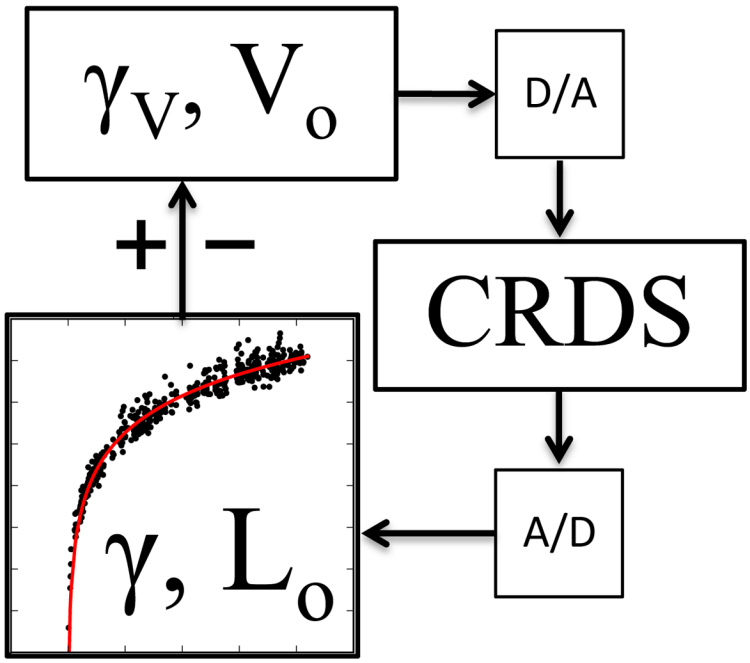

Figure 3.
Graphical Depiction of PZT control loop. Boxes with D/A and A/D signify digital to analog and analog to digital conversions respectively.

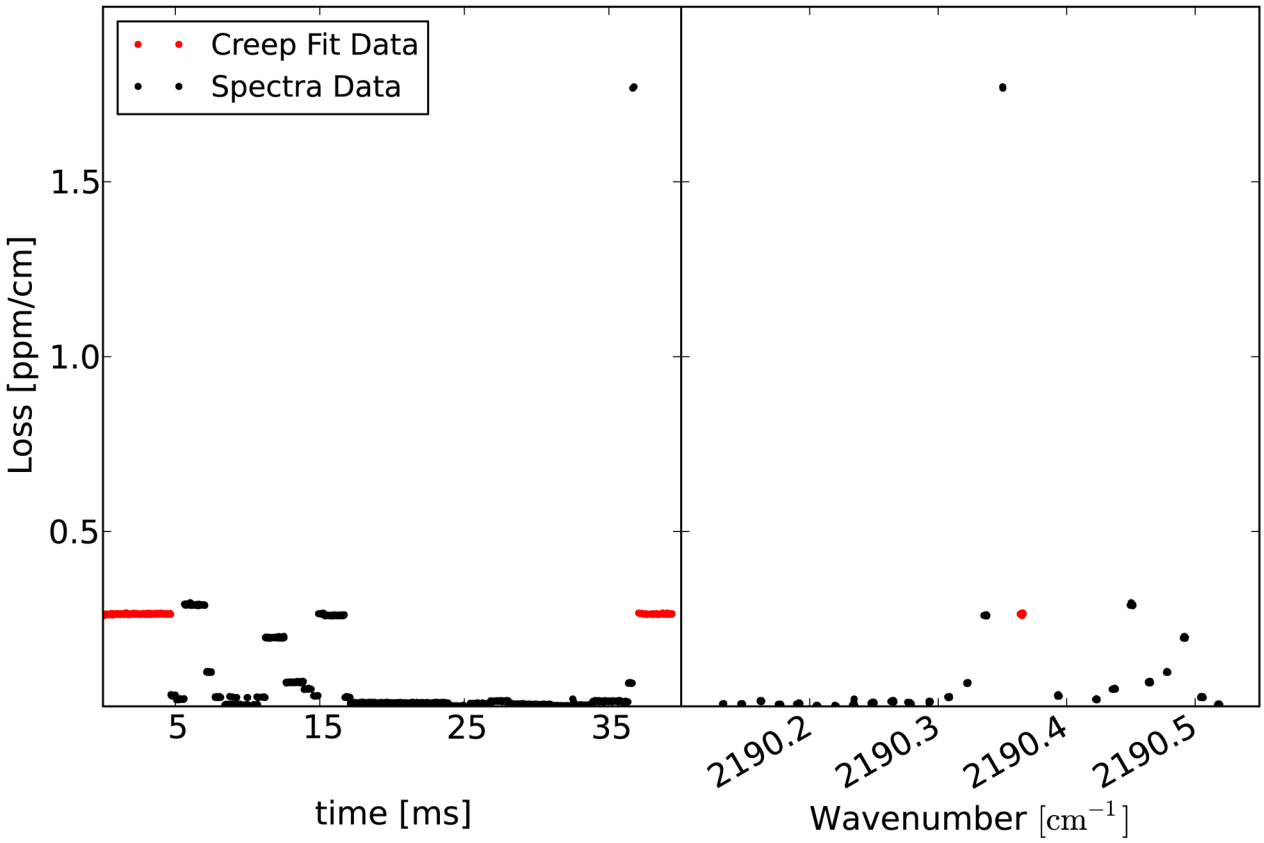

Figure 4.

Measured loss plotted versus time history and frequency for a single creep-controlled PZT voltage step. The panel to the left shows the time history of measured ring-downs with the data used to monitor PZT creep in red. The panel to the right shows the loss data plotted vs wavenumber.

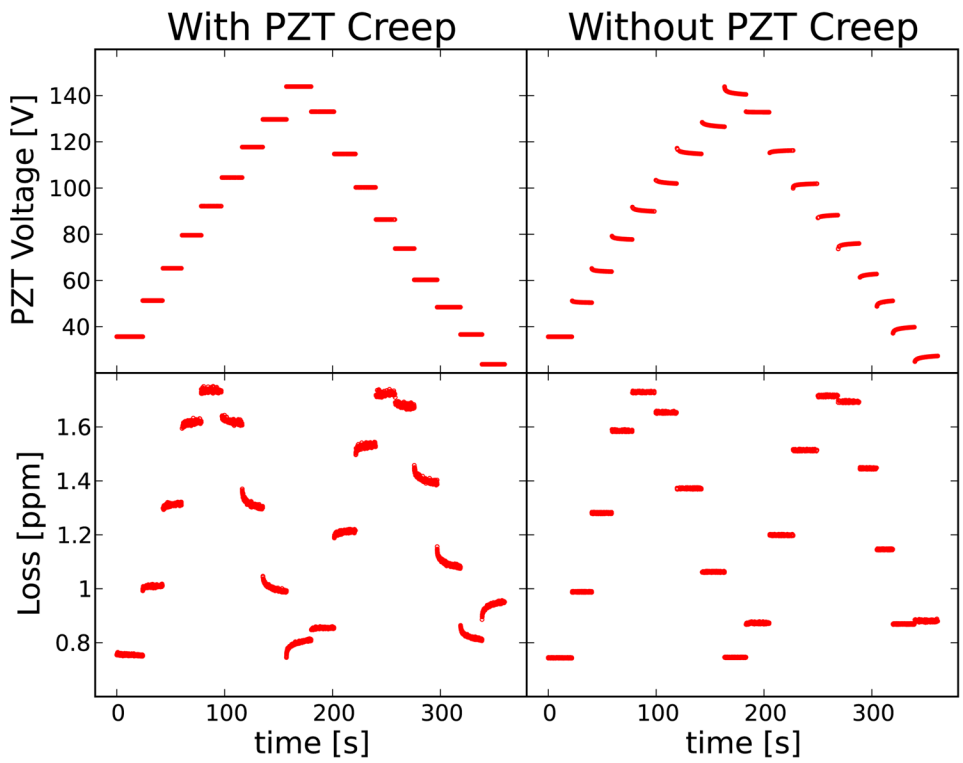

Figure 5.

PZT-voltage profiles and resultant nitrous oxide P(35) peak absorption time histories with and without PZT-creep effects. The panels on the left represent an experiment that used a simple step change voltage profile and the measured loss (lower-left) clearly shows PZT-creep effects as cavity transmission drifts over the absorption peak. The experiment depicted in the panels on the right employed a piecewise logarithmic PZT voltage function with iteratively determined PZT-creep parameters. Creep effects were effectively suppressed in the resultant loss (lower-right).

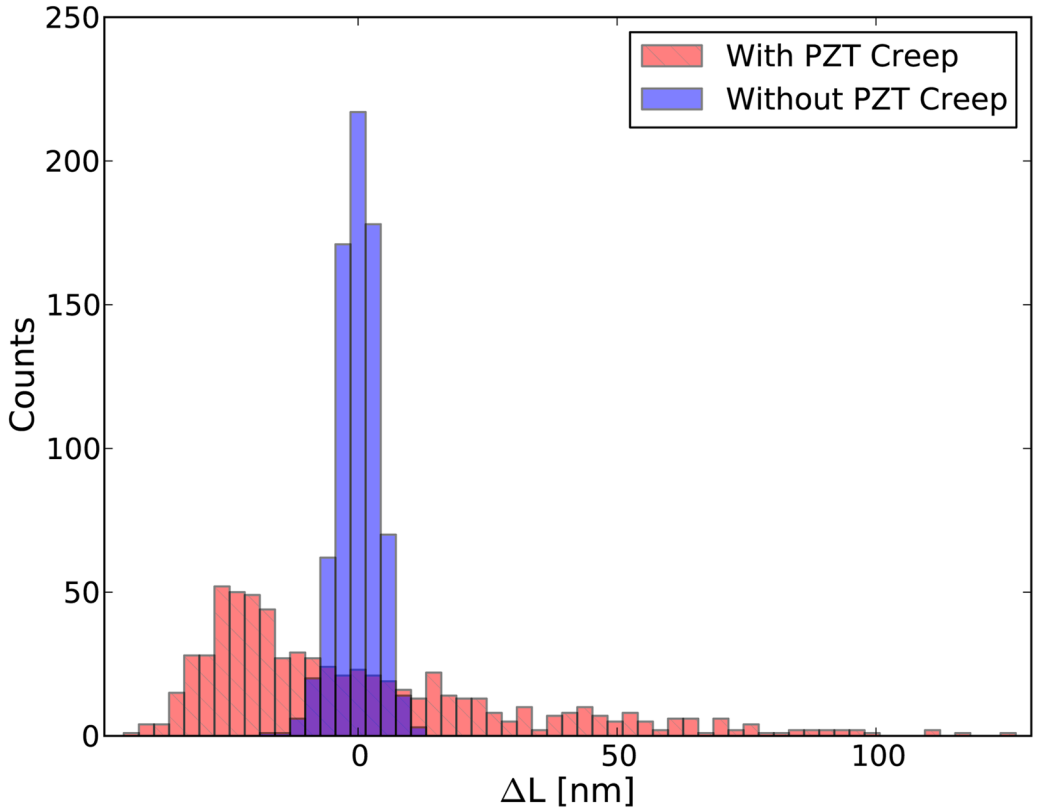

Figure 6.

Histogram of cavity length deviation from mean for one step of the voltage profile. Data acquisition routines with and without PZT creep are presented.